

## Steam explosion experiments using partially oxidized corium<sup>†</sup>

J. H. Kim<sup>\*</sup>, B. T. Min, I. K. Park, H. D. Kim and S. W. Hong

*Thermal Hydraulics Safety Research Division, Korea Atomic Energy Research Institute,  
150 Dukjin-Dong, Yusong, Taejeon, Republic of Korea 305-353*

(Manuscript Received October 17, 2007; Revised April 10, 2008; Accepted July 28, 2008)

### Abstract

Two steam explosion experiments were performed in the TROI (Test for Real cOrium Interaction with water) facility by using partially oxidized molten corium (core material), which is produced during a postulated core melt accident in a nuclear reactor. A triggered steam explosion occurred in one case, but none occurred in the other case. The dynamic pressure and the dynamic load measured in the former experiment show a stronger explosion than those performed previously with oxidic corium. Meanwhile, a steam explosion is prohibited when the melt temperature is low, because the melt is easily solidified to prevent a liquid-liquid interaction. The partially oxidized corium could enhance the strength of a steam explosion due to the thermal energy from an exothermic chemical reaction between the water and the uranium metal with a sufficient superheat extracted during melting. The melt composition effect on a steam explosion load, which was not included during the nuclear design, needs to be included in it.

*Keywords:* Steam explosion; TROI; Partially oxidized corium; Core melt accident; Nuclear reactor

### 1. Introduction

In the case of a severe accident (core melt accident) in a nuclear reactor, the reactor core may melt and interact with the coolant. Then, a rapid heat transfer from the hot melt to the surrounding cold coolant occurs with fragmentations of the melt, which leads to an explosive steam generation accompanied by destructive pressure waves—a phenomenon called a steam explosion. A steam explosion in a nuclear reactor may destroy the reactor pressure vessel and the containment to release radioactive fission products to the atmosphere. Since the TMI-II accident in the USA, a steam explosion has been one of the most important issues for a severe accident and it has been investigated extensively [1-7].

Although many achievements have been obtained from steam explosion studies, there are some remain-

ing issues such as the explosivity of a reactor core material (corium), etc. [8].

In the FARO/KROTOS experiments performed at JRC (Joint Research Center) – Ispra, no spontaneous steam explosions were observed with molten corium [4-7]. However, those experiments resulted in triggered steam explosions by applying external triggers.

Meanwhile, in the TROI (Test for Real cOrium Interaction with water) experiments performed at KAERI (Korea Atomic Energy Research Institute), the occurrence of a spontaneous or triggered steam explosion was found to be related to the composition of a corium melt [8-12].

Since a prototypic molten core material is composed of fuel (UO<sub>2</sub>), oxidized cladding material (ZrO<sub>2</sub>), unoxidized cladding material (Zr metal) and structural material (stainless steel-SS), it extracts uranium metal through a chemical reaction [13, 14], which in turn can enhance the explosivity of the corium due to the thermal energy from an exothermic chemical reaction between the extracted uranium metal and water [15].

<sup>†</sup> This paper was recommended for publication in revised form by Associate Editor Jae Young Lee

<sup>\*</sup> Corresponding author. Tel.: +82 42 868 2649, Fax.: +82 42 863 3689

E-mail address: kimjh@kaeri.re.kr

© KSME & Springer 2008

Therefore, it is necessary to perform steam explosion experiments using partially oxidized corium to establish the explosivity of a prototypic corium. In this paper, two TROI steam explosion tests (TROI-51 & 52) by using partially oxidized corium are described.

## 2. Experimental facilities

A schematic diagram of the TROI-51 experimental facilities is shown in Fig. 1.

The experimental facilities are composed of a furnace vessel (upper vessel), a pressure vessel (lower vessel), a sliding valve and an interaction vessel. The furnace and pressure vessel were designed to sustain 2.0 MPa at 212 °C. Since the furnace vessel contains a crucible in which a hot melt (~ 3000 K) would be generated by using an induction heater of 150 kW in power and 50 kHz in frequency, it was fabricated with a water jacket to protect it from the radiation heat emitted from the melt.

For the melting of the corium, a cold crucible method is introduced in this experimental series, which was originally developed by the P. N. Lebedev Physical Institute of the Academy of Sciences of the

USSR [16]. This method can be applied by flowing water into palisade-like copper tube fingers consisting of a cylindrical crucible, where the gaps between the fingers are filled with  $ZrO_2$  powder. Then the corium mixture is melted by applying an induction power and then a sintered layer of the mixture is formed between the melt and the copper fingers to prevent a leakage of the melt.

After the melt is generated and sufficiently superheated, the puncher assembly located below the cold crucible is ready to operate. The puncher assembly is composed of a water-cooled plug for blocking a hole for a melt delivery in the lower part of the cold crucible and a conical shaped puncher. When the plug is removed, the puncher perforates the melt crust formed beneath the melt to release it into the interaction vessel through a guide funnel for generating a fine jet. The sliding valve is then closed after the melt delivery to protect the crucible from a possible steam explosion.

In the pressure vessel, instrumentations are in-

Table 1. Measurement parameters and their descriptions in TROI-51.

Parameter	Sensing location	Sensor description
Melt temperature	Melt delivery path	IRCON pyrometer model 3R-35C15-0-0-1 (1500 ~ 3500 °C)
Coolant temperature	IVT101 ~ IVT106	0.5 mm, Thermocouple
Dynamic pressure in the coolant	IVDP101 ~ IVDP106	KISTLER 6005 <100 MPa
Under-water dynamic pressure	UWDP101,U WDP102	PCB model W138A26 <160 MPa
Dynamic load at the test section bottom	IVDL101	KISTLER 9081A <650 kN
Ambient temperature in the pressure vessel	PVT001 ~ PVT005	1.0 mm, Thermocouple
Static pressure in the furnace vessel	FVSP001	Rosemount model 1511 <2.0 MPa
Static pressure in the pressure vessel	PVSP004, PVSP005	Druck model PMP4060 <3.5 MPa
Dynamic pressure in the pressure vessel	PVDP004, PVDP005	KISTLER 6061B <25MPa
Melt velocity	IVT201 ~ IVT209	0.5mm, Thermocouple
Void Fraction	VFD101 ~ VFD103	Honeywell DP ST3000 STD924
Gas Sampling for Hydrogen detection	GAS005	Gas sampling bottle

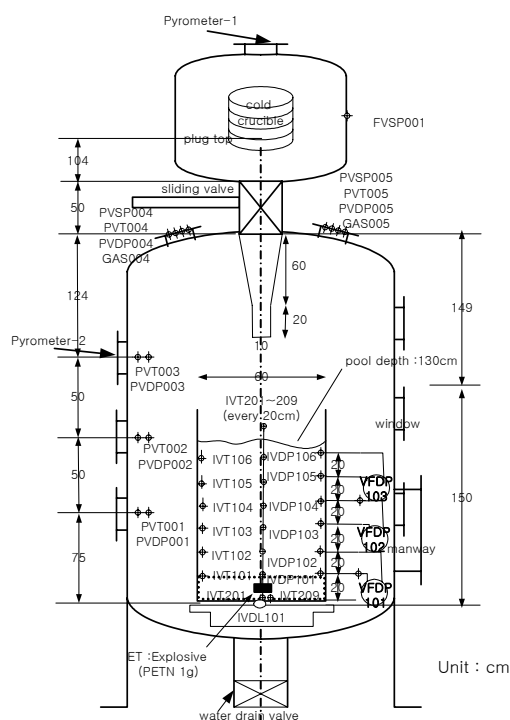


Fig. 1. Schematic diagram of TROI-51.

stalled such as temperature sensors, dynamic and static pressure gauges, gas sampling bottles and a high-speed video camera. In addition, temperature sensors, dynamic pressure transducers and a force sensor (load cell) are installed in the interaction vessel. The measurement parameters and specifications of the sensors for TROI-51 are shown in Table 1.

An optical two-color pyrometer (IRCON 3R-35C15-0-0-0-1, 1500~3500 °C, error: within 0.6% of full scale) is installed at the front of the lower vessel to direct the melt delivery path for TROI-51 and at the top of the upper vessel for TROI-52 through a viewing window to measure the melt temperature during a delivery and melting, respectively.

However, the temperature measurement is affected by a viewing tempered glass window mounted between the pyrometer and the melt in TROI-51. Therefore, the pyrometer was calibrated after the TROI-51 test. It was found that the pyrometer indicated a much higher value than the real temperature due to the glass window. The spectral transmissivity of the glass was highly dependent on the wavelength, which distorted the two-color pyrometry. The measured temperature ( $T_m$ ) through the tempered glass was calibrated in the range from 1500 °C to 2700 °C. The corrected temperature ( $T_c$ ) is shown below in Eq. (1) with respect to  $T_m$ . The temperature is in Kelvin.

$$T_c = 527.7 + 0.639 \cdot T_m \quad (1)$$

However, when the glass window is replaced by a quartz window, the measured temperature with the emissivity ratio of 0.996 is found to be the same as the reference temperature in the calibration test. Therefore, the temperature measurement in TROI-52 was performed by using a quartz window and it was not necessary to correct the measured temperature. A number of K-type thermocouples were used to measure the temperature of the water in the interaction vessel and that of the atmosphere in the pressure vessel.

Piezoelectric pressure transducers (KISTLER 6005 and PCB W138A26, maximum range of 100 MPa and 160 MPa) are mounted on the wall of the interaction vessel and in the water, respectively, to measure the dynamic pressures during a steam explosion. A load cell (KISTLER 9081A, maximum range of 650 kN) is installed beneath the interaction vessel to measure the dynamic load on the bottom of the vessel.

Three differential pressure transmitters (Honeywell

Table 2. Test conditions and results.

	TROI test number	Unit	51	52
Melt	Charge Composition	[w/o]	62.8/13.5/ 12.6/11.1	61.0/16.0/ 12.2/10.8
	UO <sub>2</sub> / ZrO <sub>2</sub> /Zr/SS			
	Measured temperature	[K]	3420	2650
	Corrected temperature	[K]	2713	2650
	Charged mass	[kg]	13.705	14.105
	Released mass	[kg]	6.309	8.604
	Initial jet diameter	[cm]	10	5
	Free fall in gas	[m]	3.2	3.2
Test	Water mass	[kg]	367	367
Section	Initial height	[m]	1.3	1.3
	Final height	[m]	1.02	1.23
	Cross section	[m <sup>2</sup> ]	0.283	0.283
	Initial temp.	[K]	294	285
	Sub-cooling	[K]	79	88
Pressure	Initial pressure	[MPa]	0.115	0.116
Vessel	Initial temp.	[K]	297	289
	Free volume	[m <sup>3</sup> ]	8.023	8.023
Results	Maximum PV pressurization	[MPa]	0.053	0.070
	Time to reach peak	[s]	3.2	3.0
	PV heat-up	[K]	53	276
	Time to stabilize	[s]	6	10
	Water heat-up	[K]	5	10
	Time to stabilize	[s]	11	18
	Steam explosion		Yes	No
	Triggering (ET) time after melt delivery	[s]	1.35	1.67
	Dynamic pressure	[MPa]	32 (SE)	11 (ET)
	Duration	[ms]	1.1 (SE)	1.2 (ET)
	Impulse	[kN]	580 (SE)	275 (ET)
	Duration	[ms]	11 (SE)	9 (ET)
Debris	Total	[kg]	6.309	8.604
	> 6.35 mm	[kg]	0.595	0.510
	4.75 ~ 6.35 mm	[kg]	0.400	1.005
	2.0 ~ 4.75 mm	[kg]	1.355	3.645
	1.0 ~ 2.0 mm	[kg]	1.075	1.835
	0.71 ~ 1.0 mm	[kg]	0.450	0.515
	0.425 ~ 0.71 mm	[kg]	0.700	0.555
< 0.425 mm	[kg]	1.734	0.539	

DP ST3000 STD924) measure the void fractions in the water by using a swelling level due to the voids.

An external trigger (Explosive PETN, 1 g) is installed at the bottom of the water in the test section. The explosive is installed at 65 mm above the bottom of the rigid cylindrical interaction vessel of 0.6 m in diameter to trigger a steam explosion. Static pressure transducers measure the transient pressure in the pressure vessel and the furnace vessel. A VXI system

(sampling rate per channel : 800 kHz for dynamic signal measurement and 1 kHz for steady signal measurement) manufactured by Agilent Technology is used for the data acquisition.

### 3. Experimental results

Two TROI steam explosion tests of TROI-51 and 52 were performed to investigate the effect of partially oxidized corium on the occurrence of a steam explosion. By the time for the melt to hit the bottom of the water-filled interaction vessel, an external trigger (ET) was applied to induce an explosion.

The initial conditions and results of the TROI-51 and 52 tests are shown in Table 2. The test section of 0.6 m in diameter was filled with 1.3 m deep water, which was at room temperature and almost at atmospheric pressure. An external trigger (ET) was applied at 1.35 s in TROI-51 and 1.67 s in TROI-52, but the error range of the trigger unit and DAS produced slight time differences.

#### 3.1. TROI-51 test results

This test was carried out to induce a triggered steam explosion with partially oxidized corium. Since the partially oxidized corium extracted a uranium metal layer in the form of  $UFe_2$  [14], the effect of the extracted uranium metal on the energetics of a triggered steam explosion was examined.

The mixture of  $UO_2$ ,  $ZrO_2$ , Zr and stainless steel was charged into the crucible at a weight percent of 62.8, 13.5, 12.6 and 11.1 %, respectively. This percentage was referred to from the MASCA project [13]. Then the mixture was melted and the molten corium was delivered into the water in the interaction

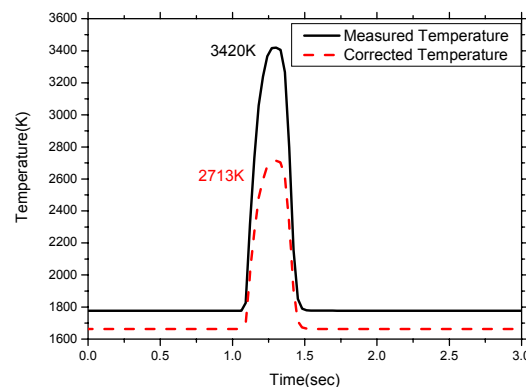


Fig. 2. Melt temperature during delivery in TROI-51.

vessel. The melt just before a melt delivery would be composed of a metallic layer of  $UFe_2$  and an oxidic layer of  $ZrO_2$  since the initial composition was almost similar to that of the previous tests [14].

During the melt delivery, the melt temperature was measured at the exit of the guide funnel, and it is presented in Fig. 2. The maximum melt temperature measured through the tempered glass window was 3420 K. The corrected temperature was 2713 K after compensation for the glass window.

When the melt jet penetrated the water in the interaction vessel, an external trigger was applied at 1.35 seconds after the initiation of the melt delivery, which is the time of a puncher actuation.

Fig. 3 shows the dynamic pressures in the water measured by the wall-mounted pressure sensors. It shows two peaks at about 1.327 s and 1.329 s. The first peak shows a propagation of the pressure waves from the bottom (IVDP101) to the top (IVDP104).

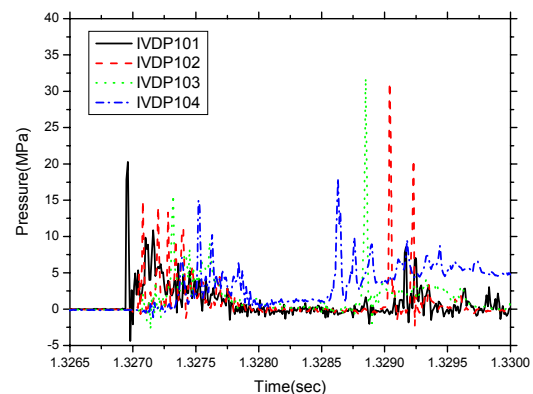


Fig. 3. Dynamic pressures from wall-mounted sensors in TROI-51.

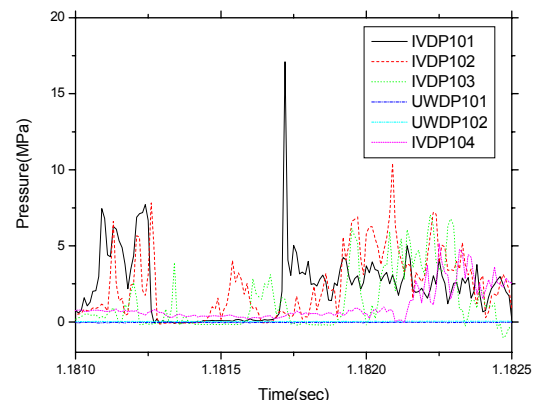


Fig. 4. Dynamic pressures from the previous test with oxidic corium (TROI-36).

This peak is caused by an external trigger located at the bottom. The second peak shows another propagation from the top to the bottom. It is believed that a steam explosion was induced by the external trigger when the melt front was still at the top of the water. The magnitude of the pressure by the steam explosion was 32 MPa, which is higher than those (~ 20 MPa) from the previous TROI tests with oxidic corium. The dynamic pressures from a strong steam explosion with oxidic corium among the previous tests [12] are presented in Fig. 4. Sensor locations are the same as TROI-51.

Fig. 5 shows the dynamic pressures in the water measured by under-water sensors. It shows a similar pattern to those from the wall-mounted sensors. However, the magnitude was much smaller. This is probably caused by the movement of the sensors at the time of the explosions since the sensors were not fixed. The duration was 1.1 ms, similar to the signals from the wall-mounted sensors.

Fig. 6 shows the dynamic load on the bottom of the interaction vessel. The maximum value was quite high at 580 kN, which is much stronger than those (~ 300 kN) from the previous tests with oxidic corium. The dynamic load from a strong steam explosion with oxidic corium among the previous tests [12] is presented in Fig. 7. The present test shows much higher load than the previous test with oxidic melt.

From Fig. 6, the external triggering was initiated at 1.327 seconds after the puncher actuation. The duration of the steam explosion was 11 ms, which is similar to the previous steam explosion tests. From this signal, a triggered steam explosion is believed to have occurred.

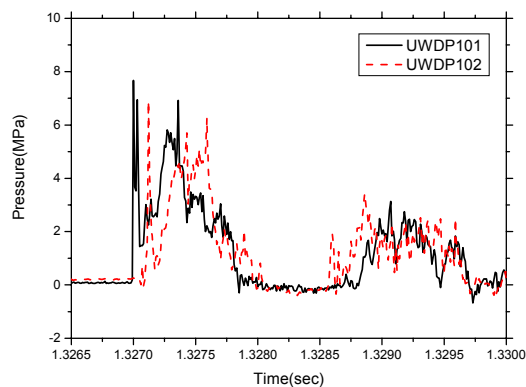


Fig. 5. Dynamic pressures from under-water sensors in TROI-51.

Fig. 8 shows the debris size distribution after the TROI-51 test. This figure shows that the mass fraction of the fine particles, smaller than 0.425 mm, is 27.5 %. This is a big amount when compared with non-explosive tests (less than 10 %) [17]. Furthermore, the mass mean diameter is as small as 1.2 mm.

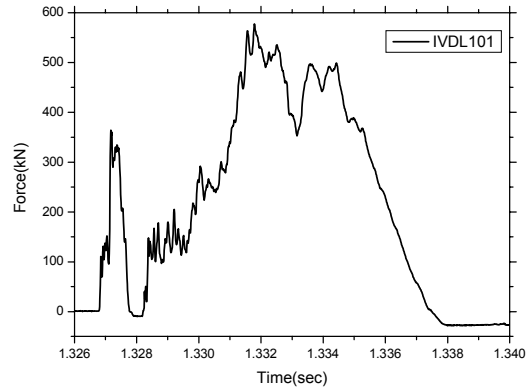


Fig. 6. Dynamic load in TROI-51.

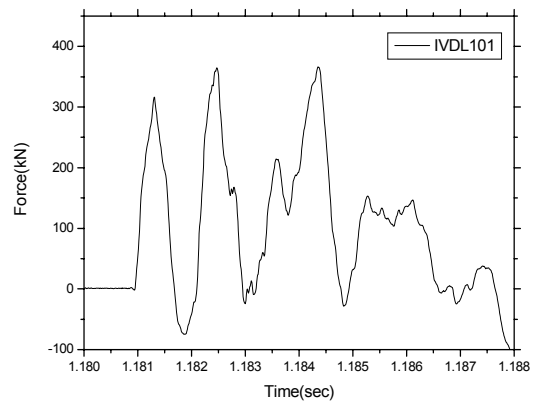


Fig. 7. Dynamic load from the previous test with oxidic corium (TROI-36).

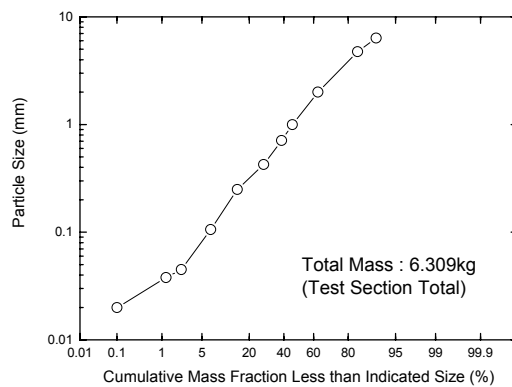


Fig. 8. Debris size distribution in TROI-51.

From these facts, a steam explosion was triggered in this test, by fragmenting the molten corium into fine particles, which led to a rapid pressure increase due to an explosive steam generation.

Fig. 9 shows a microscopic image of the fine debris. Most of it is highly porous and irregular. When the debris has a significant amount of metallic components, the shape of the debris is somewhat similar to that of metallic melts [18]. The shape of metallic debris under a fast quenching is far from a sphere, due to the high thermal conductivity of metal. The solidification of the metallic portion of the debris would be fast, while the oxidic portion is still a liquid [19]. Meanwhile, the compositions of debris are also seen to be very non-homogeneous as shown in Fig. 10. This figure shows the compositions along the cross section for the debris ‘c’ in Fig. 9. The non-homogeneity of the debris could be caused by the different solidification behaviors between the metals and oxides aforementioned.

Meanwhile, since the chemical reaction between the extracted uranium metal and water is exothermic,

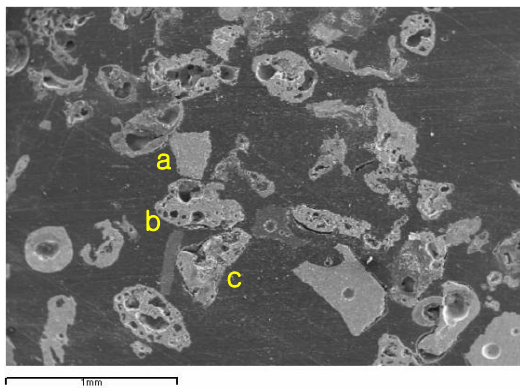


Fig. 9. Morphology of debris in TROI-51.

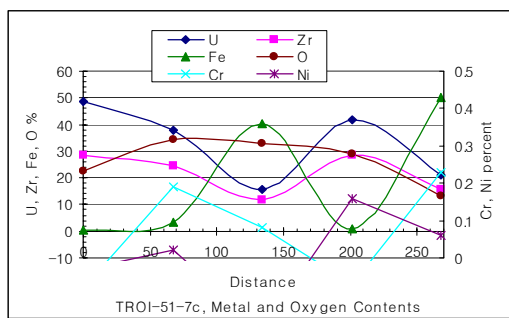


Fig. 10. Chemical composition along the cross section for debris from TROI-51.

it releases oxidation energy. Therefore, a steam explosion with partially oxidized corium is stronger than that with oxidic corium due to this exothermic reaction energy, when an explosion is triggered [15]. For this reason, a relatively strong steam explosion occurred in TROI-51.

3.2. TROI-52 test results

This test was performed to repeat the TROI-51 test. The weight percentages of the charged material were slightly changed. The weight percentage of UO<sub>2</sub>, ZrO<sub>2</sub>, Zr and stainless steel was 61.0, 16.0, 12.2 and 10.8 %, respectively. Then the mixture was melted in the cold crucible.

The melt temperature was measured by using a pyrometer through a quartz viewing glass, so there was no need to compensate for the glass window. The melt temperature measured during the melting is presented in Fig. 11. The temperature reached 2650 K, which is much lower than that in TROI-51. After melting for 5860 seconds, the melt was delivered into the water through a guide funnel.

Figs. 12 and 13 show the dynamic pressures in the water measured by the wall-mounted pressure sensors and those by the under-water pressure sensors, respectively. They only show one peak at about 1.715 s. This peak shows a propagation of pressure waves from the bottom to the top. This peak is caused by an external trigger (ET) located at the bottom. The error range of the trigger unit and DAS caused a slightly later triggering than the preset time of an external trigger (1.67 seconds). Therefore, no steam explosion is claimed to have been induced. The reason for no steam explosion is the low melt temperature (super

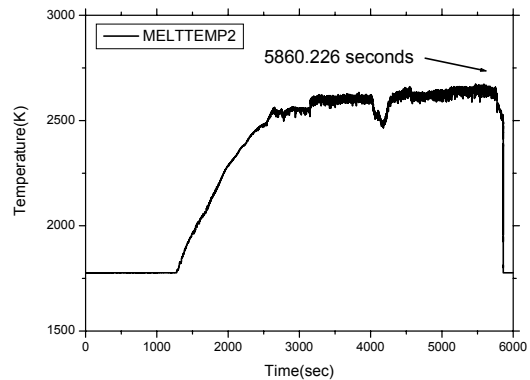


Fig. 11. Melt temperature during melting in TROI-52.

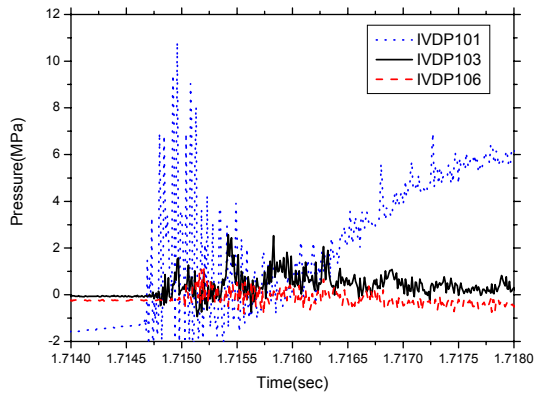


Fig. 12. Dynamic pressures from wall-mounted sensors in TROI-52.

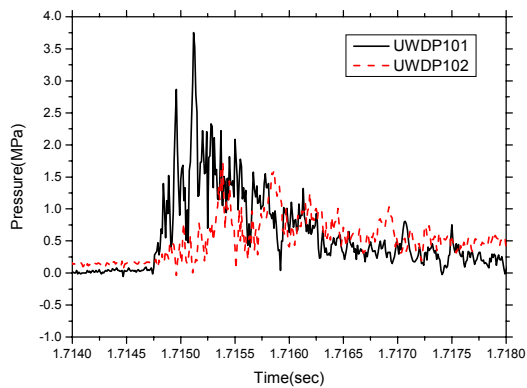


Fig. 13. Dynamic pressures from under-water sensors in TROI-52.

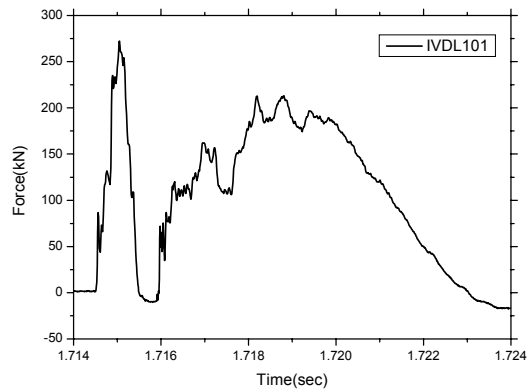


Fig. 14. Dynamic load in TROI-52.

heat). Since the melt can be solidified easily during its penetration through the water, no liquid – liquid contact occurred at the time of an external triggering.

Fig. 14 shows the dynamic load on the bottom of

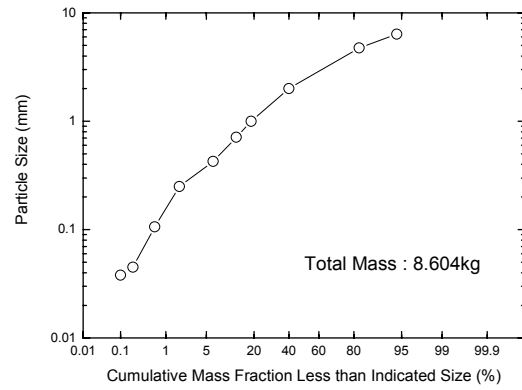


Fig. 15. Debris size distribution in TROI-52.

the interaction vessel. It shows a much smaller peak value than TROI-51, which indicates no steam explosion.

After the test, the debris was collected and sieved. The classified debris size distribution is presented in Fig. 15. The mass fraction of the fine particles, smaller than 0.425 mm, is 6.3 %. The mass mean diameter is 2.6 mm. Compared to TROI-51, these values confirm no occurrence of a steam explosion. As no fine fragmentation occurred, a rapid heat transfer leading to a steam explosion was not induced in this test.

#### 4. Conclusions

Two TROI steam explosion tests have been performed by using partially oxidized corium melt. One led to a strong steam explosion by applying an external trigger, when the melt temperature was sufficiently high. The other did not lead to a triggered steam explosion, when the melt temperature was not high enough. Fine fragmentations essential for a steam explosion were not achieved with the melt at a low temperature, due to a solidification of the melt during an interaction between the melt and coolant. With a high melt temperature, the melt was finely fragmented and steam was explosively generated. The explosivity of the partially oxidized corium was found to be higher than that of the oxidic corium. The partially oxidized corium could enhance the strength of a steam explosion due to the thermal energy from an exothermic chemical reaction between the water and the uranium metal with a sufficient superheat extracted during melting. Therefore, the melt composition effect on a steam explosion load which was not

included during a nuclear design needs to be included in it. More steam explosion tests with partially oxidized corium need to be performed to confirm its high explosivity.

### Acknowledgments

This study has been carried out under the nuclear R&D program by the Korean Ministry of Science and Technology.

### Nomenclature

$T_c$  : Corrected temperature after calibration (K)  
 $T_m$  : Measured temperature (K)

### References

- [1] D. E. Mitchell, M. L. Corradini and W. W. Tarbell, *Intermediate scale steam explosion phenomena: Experiments and analysis*, SAND81-0124, SNL, USA, (1981).
- [2] N. Yamano, Y. Maruyama, T. Kudo, A. Hidaka and J. Sugimoto, Phenomenological studies on melt-coolant interactions in the ALPHA program, *Nuclear Engineering and Design*, 155 (1995) 369-389.
- [3] D. H. Cho, D. R. Armstrong and W. H. Gunther, *Experiments on interactions between zirconium-containing melt and water*, NUREG/CR-5372 (1998).
- [4] D. Magallon, I. Huhtiniemi and H. Hohmann, Lessons learnt from FARO/TERMOS corium melt quenching experiments, *Nuclear Engineering and Design*, 189 (1999) 223-238.
- [5] D. Magallon and I. Huhtiniemi, Corium melt quenching tests at low pressure and subcooled water in FARO, *Nuclear Engineering and Design*, 204 (2001) 369-376.
- [6] I. Huhtiniemi, D. Magallon and H. Hohmann, Results of recent KROTOS FCI tests: alumina versus corium melts, *Nuclear Engineering and Design*, 189 (1999) 379-389.
- [7] I. Huhtiniemi and D. Magallon, Insight into steam explosions with corium melts in KROTOS, *Nuclear Engineering and Design*, 204 (2001) 391-400.
- [8] J. H. Song, I. K. Park, Y. J. Chang, Y. S. Shin, J. H. Kim, B. T. Min, S. W. Hong and H. D. Kim, Experiments on the interactions of molten  $ZrO_2$  with water using TROI facility, *Nuclear Engineering and Design*, 213 (2002) 97-110.
- [9] J. H. Kim, I. K. Park, B. T. Min, S. W. Hong, J. H. Song and H. D. Kim, An effect of corium composition variations on occurrence of a spontaneous steam explosion in the TROI experiments, *Proceedings of NUTHOS-6*, Nara, Japan, October 4 ~ 8 (2004).
- [10] J. H. Kim, I. K. Park, B. T. Min, S. W. Hong, H. Y. Kim, J. H. Song and H. D. Kim, Triggered steam explosion experiments in the TROI facility, *Proceedings of International Congress on Advanced Nuclear Power Plant (ICAPP'05)*, Seoul, Korea, May 15-19 (2005).
- [11] J. H. Kim, I. K. Park, B. T. Min, S. W. Hong, S. H. Hong, J. H. Song and H. D. Kim, Results of the triggered TROI steam explosion experiments with a narrow interaction vessel, *Proceedings of International Congress on Advanced Nuclear Power Plant (ICAPP'06)*, Reno, NV, USA, June 4-8 (2006).
- [12] J. H. Kim, I. K. Park, B. T. Min, S. W. Hong, S. H. Hong, J. H. Song and H. D. Kim, Results of the triggered steam explosions from the TROI experiment, *Nuclear Technology*, 158 (3) (2007) 378-395.
- [13] V. Asmolov and V. Strizhov, Overview of the progress in the OECD MASCA project, *Cooperative Severe Accident Research Program (CSARP) Meeting*, Washington DC, USA (2004).
- [14] J. H. Kim, B. T. Min, S. W. Hong, S. H. Hong, I. K. Park, J. H. Song and H. D. Kim, Layer inversion tests with metal-added corium in the TROI experiment, *Proceedings of ICAPP'07*, Nice, France, May 13-18 (2007).
- [15] M. Leskovar, R. Meignen, C. Brayer, M. Burger and M. Buck, Material influence on steam explosion efficiency: state of understanding and modeling capabilities, *2<sup>nd</sup> European Review Meeting on Severe Accident Research (ERMSAR-2007)*, FZK, Germany, June 12-14 (2007).
- [16] V. I. Aleksandrov, V. V. Osiko, A. M. Prokhorov and V. M. Tatarntsev, Chapter 6, Synthesis and crystal growth of refractory materials by RF melting in a cold container, *Current Topics in Materials Science*, Vol. 1, Edited by E. Kaldis, North-Holland Publishing Company (1978).
- [17] I. K. Park, J. H. Kim, S. H. Hong, B. T. Min, S. W. Hong, J. H. Song, and H. D. Kim, An investigation of the particle size responses for various fuel-coolant interactions in the TROI experiments, *Nuclear Technology*, 161 (2008) 45-56.
- [18] L. C. Witte, T. J. Vyas and A. A. Gelabert, Heat transfer and fragmentation during molten-metal/



water interactions, *Journal of Heat Transfer*, 95 (4) (1973) 521-527.

- [19] J. H. Song, B. T. Min, B. T. and F. Defoort, The effect of a material composition on the strength of a prototypic steam explosion, *Proceedings of NTHAS5*, Jeju, Korea, Nov. 26-29 (2006).



**Jong-Hwan Kim** is a principal researcher at Thermal Hydraulics Safety Research Division at Korea Atomic Energy Research Institute (KAERI). He received B.Sc. and M.Sc. degrees with nuclear engineering from Seoul National University

in the Republic of Korea and a Ph.D. degree with film boiling heat transfer in 1994 from the University of Manchester in the United Kingdom. Thereafter, he has been working on the safety research for the severe accidents at nuclear power plants, especially fuel-coolant interactions.